Proc. Natl. Acad. Sci. USA
Vol. 79, pp. 4632–4636, August 1982
Biophysics

Anisotropic magnetic interactions in the primary radical ion-pair of photosynthetic reaction centers

(photosynthesis/bacteriochlorophyll/magnetic field effect)

STEVEN G. BOXER, CHRISTOPHER E. D. CHIDSEY, AND MARK G. ROELOFS

Department of Chemistry, Stanford University, Stanford, California 94305

Communicated by Gerhard Closs, March 15, 1982

ABSTRACT **The quantum yield of triplets formed by ion-pair recombination in quinone-depleted photosynthetic reaction centers is found to depend on their orientation in a magnetic field. This new effect is expected to be a general property of radical pair reactions in the solid state. For $0 < H < 1{,}000$ G, the quantum yield anisotropy is caused by anisotropic electron dipole–electron dipole or nuclear hyperfine interactions, or both. For high fields it is dominated by the anisotropy of the difference *g*-tensor in the radical ion-pair. The magnitude and sign of the contribution of each interaction depend not only on the values of the principal components of each anisotropic tensor but also on the geometric relationship of the principal axes of each tensor to the transition dipole moment used to detect the yield. A detailed formalism is presented relating these quantities to the observed yield anisotropy. The expected magnitude of each anisotropic parameter is discussed. It is demonstrated that the field dependence of the yield anisotropy is consistent with these values for certain reaction center geometries.**

Although our knowledge of the kinetics of the primary events in bacterial photosynthesis is sophisticated, basic structural questions—such as the distance between the primary electron donor (P) and acceptor (I), the direction of electron flow relative to the photosynthetic membrane surface, and the absolute orientations of the reactive components—remain unanswered. The difficulty, of course, is that the photosynthetic reaction center (RC) is a membrane-bound chromophore–protein complex and thus far has not been studied by single-crystal x-ray diffraction. This problem is not unique to photosynthesis and many of these same questions apply to other membrane-bound energy-transducing complexes (e.g., purple membranes, Na^+/K^+ ATPases, cytochrome oxidase).

The molecular triplet state of the primary electron donor is formed by recombination of the primary radical ion-pair, $P^{+}I^{-} \rightarrow {}^3PI$, in bacterial RCs depleted of secondary electron acceptors (see Fig. 1) (1, 2). In the present paper we demonstrate that the quantum yield of this triplet state, Φ_T, depends on the orientation of the RCs in a magnetic field. We suggest that this effect is due to anisotropic magnetic interactions in the initial radical ion pair ($P^{+}I^{-}$). Because of the straightforward dependence of such interactions on structure, this observation can contribute a great deal to our understanding of the basic questions posed above. In general, we expect that the quantum yield of radical ion-pair reactions in rigid media will depend on the orientation of the species in a magnetic field and that the interpretation of this dependence can lead to structural information.

The quantum yield of ^3P in RCs as a function of the applied magnetic field strength, $\Phi_T(H)$, has been studied by a number of investigators. $\Phi_T(H)$ is observed to decrease in the range 0–500 G (3, 4) and to increase again over the range 2–50 kG, becoming independent of field at very high field with a value in excess of the zero-field yield (5, 6). These observations are explained by the spin dynamics of the radical ion pair, $P^{+}I^{-}$, in competition with the recombination reactions. In small fields the loss of degeneracy of the singlet radical pair state, S, with two of the triplet radical pair states, T_+ and T_-, decreases the rate of triplet radical pair formation (7, 8). In large fields, the difference in the *g*-factors of the radicals can contribute enough to the rate of T_0 radical pair formation to make up for the loss at low field, such that the Φ_T at high field exceeds that at zero field. At very high fields, the yield of ^3P reaches a plateau because the rapid rate of $S–T_0$ interconversion brings the two radical pair states into equilibrium prior to recombination (6).

In the high-field limit (electron Zeeman interaction much greater than the spin-spin interactions, $H > 300$ G), the radical-pair energy-level diagram reduces to a simple two-level system, S and T_0. The splitting of these two states is due to the isotropic exchange interaction and the anisotropic electron dipole–electron dipole fine structure interaction which depends on the orientation of $P^{+}I^{-}$ in the magnetic field. Because $\Phi_T(H)$ depends explicitly on the singlet–triplet splitting which impedes $S–T_0$ mixing, RCs with different orientations in a magnetic field should have different triplet quantum yields. In addition, the nuclear hyperfine interactions and the *g*-factor difference which drive $S–T_0$ mixing may be anisotropic. Because the contribution of the *g*-factor difference to the rate of $S–T_0$ mixing increases with increasing field, whereas that due to hyperfine interactions and the inhibition due to the dipole–dipole interaction are constant with field strength, the anisotropy of Φ_T may change dramatically with field. We have shown elsewhere (5, 6) that, in the high-field limit and for isotropic interactions, $\Phi_T(H)$ has a relatively simple theoretical form. It is shown in this paper that this relationship also is valid for anisotropic interactions when it is recognized that various parameters are functions of the orientation of the RC in the magnetic field.

EXPERIMENTAL

In this experiment we probe the absorption of P at 870 nm with light polarized either parallel or perpendicular to the magnetic field. The absorption is probed after $P^{+}I^{-}$ has completely decayed but before ^3P has decayed to any significant extent. Thus, we select for observation an anisotropic distribution of RCs; if the yield of ^3P is anisotropic, we can observe an anisotropic bleach of P absorption (Fig. 1). The excitation and observation beams are directed at a right angle to the field by using mirrors within the magnet bore (9). Quinone-depleted (10) RCs (10 μM) in a viscous solvent [a mixture of 33% (vol) 20 mM Tris·HCl/

The publication costs of this article were defrayed in part by page charge payment. This article must therefore be hereby marked "*advertisement*" in accordance with 18 U. S. C. §1734 solely to indicate this fact.

Abbreviation: RC, reaction center.

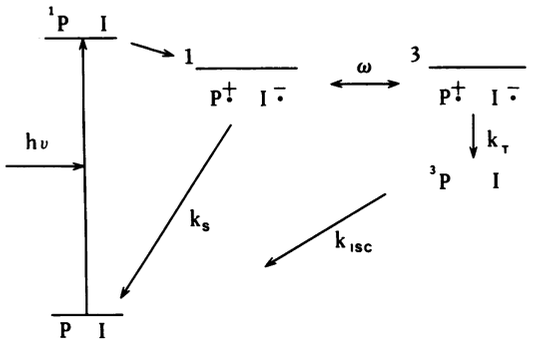

FIG. 1. Simplified scheme for the primary events in quinone-depleted RCs. k_S and k_T are the singlet and triplet radical-pair recombination rate constants; ω is the singlet–triplet mixing frequency which depends on the magnetic parameters for the radical pair and the field strength. The bar above P^+I^- denotes a spin-correlated radical pair.

10 μM EDTA/0.05% Triton X-100, pH 8.0 and 67% glycerol] are held in a 1-mm cuvette at room temperature. The RCs are not oriented (see *Results*). They are excited at 532 nm with the electric polarization vector of the subsaturating 8-ns pulse at angle η_e to the applied magnetic field, $\vec{H}$. At 3 μs later, the change in P absorption at 870 nm, $S(H,\eta_e,\eta_o)$, is measured with the electric polarization vector of the observation light at the angle η_o to $\vec{H}$. The polarization direction of one of the beams is varied at zero field to determine the small amount of photoselection: $S(0,0°,0°)/S(0,0°,90°) = 1.035 \pm 0.006$. The polarization directions of both beams are varied at zero field to determine the instrumental artifact: $[S(0,0°,0°)/S(0,0°,90°)] - [S(0,90°,90°)/S(0,90°,0°)] = -0.007 \pm 0.008$.

RESULTS

In a magnetic field, the effect of varying the polarization of the observation beam, η_o, is large and highly field dependent (Fig. 2). This result implies both a highly anisotropic quantum yield and a highly anisotropic absorption at 870 nm. The effect of varying the polarization of the excitation pulse, η_e, is much smaller. Table 1 shows these effects for a set of experiments at 1 and 50 kG. This table contains the observation and excitation anisotropies, $a_o(H,\eta_e)$ and $a_e(H,\eta_o)$, that are obtained from the relative yields, $I(H,\eta_e,\eta_o)$:

$$I(H,\eta_e,\eta_o) = S(H,\eta_e,\eta_o)/S(0,\eta_e,\eta_o) \quad [1]$$

$$a_o(H,\eta_e) = \frac{I(H,\eta_e,0°) - I(H,\eta_e,90°)}{I(H,\eta_e,0°) + 2\,I(H,\eta_e,90°)} \quad [2]$$

$$a_e(H,\eta_o) = \frac{I(H;0°,\eta_o) - I(H,90°,\eta_o)}{I(H,0°,\eta_o) + 2\,I(H,90°,\eta_o)}. \quad [3]$$

Because the relative yields, $I(H,\eta_e,\eta_o)$, are defined as ratios, the effect of the field-independent photoselection is not included in either of the anisotropies, and $a_o(0,\eta_e) = a_e(0,\eta_o) \equiv 0$.

If absorption at 532 nm were isotropic, the observation anisotropy, $a_o(H,\eta_e)$, would be independent of η_e and the excitation anisotropy, $a_e(H,\eta_o)$, would be zero at all fields. Both of these conditions are approximately satisfied by the data in Table 1. An alternative, but far less likely, possibility is that the transition dipole moment at 532 nm is well defined but lies near the "magic angle" (54.74°) to the principal axes of each significant anisotropic interaction and also to the transition dipole moment at 870 nm (necessary to explain the weak photoselection). We discard this possibility as extremely unlikely and, in the discussion which follows, will take the excitation to be isotropic due to the diversity of transitions at 532 nm. Thus, we consider only the observation angle and make the replacements:

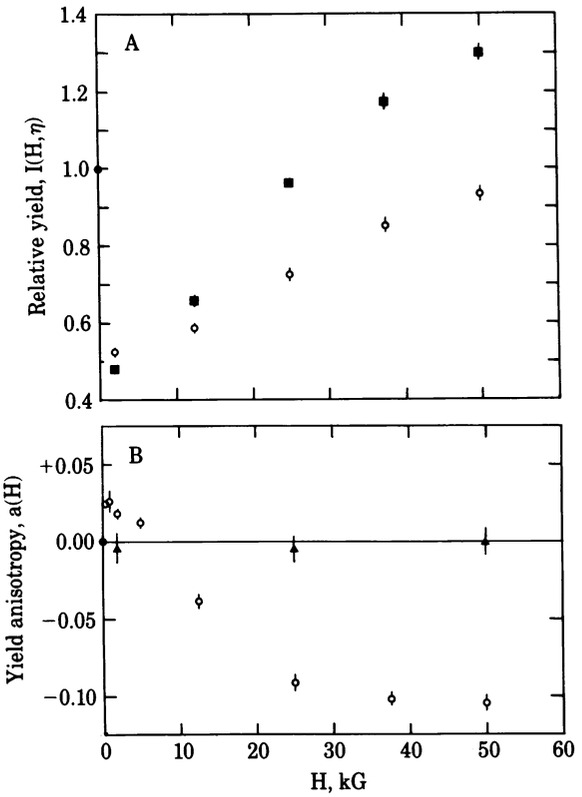

FIG. 2. Relative quantum yield, $I(H,\eta)$, as a function of magnetic field for quinone-depleted RCs at 293 K in viscous glycerol/buffer. $\eta = 0°$, ○; $\eta = 90°$, ■. (*B*) Quantum yield anisotropy, a(H), as a function of magnetic field in viscous glycerol/buffer (○) and in nonviscous buffer (▲). $I(H,\eta)$ and a(H) are defined in Eq. 4.

$$\eta = \eta_o,\ I(H,\eta) = I(H,\eta_e = 0°,\ \eta_o), \quad [4]$$

and

$$a(H) = a_o(H,\eta_e = 0°).$$

The quantum yield at zero field, $\Phi_T(0)$, has been measured (9, 11). The average quantum yield, $\Phi_T^{av}(H)$, at any field can be calculated:

$$\Phi_T^{av}(H) = \Phi_T(0)(1/3)[I(H,0°) + 2\,I(H,90°)]. \quad [5]$$

A plot of the relative yields, I(H,0°) and I(H,90°), as a function of field and the quantum yield anisotropy, a(H), are shown in Fig. 2. The extraordinary observation that a(H) is positive at low fields and negative at high fields indicates that there are two or more anisotropic magnetic interactions contributing to the yield anisotropy. $I(H,\eta)$ has been measured as a function of the angle η and fits well to the expected function, $1/3\,[I(H,0°) + 2\,I(H,90°)][1 + a(H)(3\cos^2\eta - 1)]$. When the RCs are suspended in buffer with no glycerol at room temperature, a(H)

Table 1. Excitation and observation anisotropies*

	H = 1 kG	H = 50 kG
$a_o(H,0°)$	+0.024 ± 0.009	−0.117 ± 0.010
$a_o(H,90°)$	+0.023 ± 0.009	−0.114 ± 0.010
$a_e(H,0°)$	+0.000 ± 0.009	−0.011 ± 0.005
$a_e(H,90°)$	−0.005 ± 0.009	−0.011 ± 0.005

* Calculated by using Eqs. 2 and 3. Values are mean ± SD.

$= 0.00 \pm 0.01$ for all fields (Fig. 2*B*). This is a consequence of complete rotational "depolarization" of the yield anisotropy during the 3 μsec following the excitation flash (the rotational correlation time for the 100-kdalton RC complex is on the order of hundreds of nanoseconds in a solvent with a viscosity of 1 cp). The lack of anisotropy in nonviscous solution demonstrates that the anisotropy observed in viscous solutions is chemically induced anisotropy and is not due to an equilibrium orientation of the RC particles by the field. Finally, a(H) was measured as a function of time after the flash in viscous solution to demonstrate that a(H) does not decay significantly in 3 μsec.

DISCUSSION

The anisotropy observed in these measurements is due to the magnitudes of the anisotropic magnetic interactions in $P^{+}I^{-}$. In the following section we develop theoretical expressions for $\Phi_T^{av}(H)$ and a(H).

The following notation is used. The laboratory-fixed axis system is designated by the unit vectors: $\hat{x}$, $\hat{y}$, and $\hat{z}$, with the magnetic field in the $\hat{z}$ direction. The RC-fixed axis system is designated by $\hat{a}$, $\hat{b}$ and $\hat{c}$. The c axis is defined to lie along the transition dipole moment direction at 870 nm, $\hat{\mu}_{870}$. The RC axis system is related to the laboratory axis system by the Euler angles α, β, and γ(12). The principal axes of the tensors describing the anisotropic magnetic interactions are $\hat{x}_i$, $\hat{y}_i$, and $\hat{z}_i$, where i is D for the electron dipole–electron dipole tensor, A for nuclear hyperfine tensors, P for nuclear quadrupole tensors, or g for the difference g-tensor between P^{+} and I^{-}. The orientation of the principal axis system of each anisotropic interaction with respect to the RC axis system is described by the three Euler angles α_i, β_i, and γ_i. These are fixed by the structure of the RC, and contain the structural information we desire. (The choice of one of the α_is is arbitrary and defines the a-axis of the RC axis system.) For simplicity, we adopt the following truncated subscript notation: the components of a tensor in its principal axis system are denoted with single subscripts, as in A_x, A_y, and A_z for the principal values of the hyperfine tensor, and the components in the laboratory axis system by the standard double subscript, as in A_{zz}.

In order to model the data, we must calculate the yield, $\Phi_T(\beta,\gamma)$, for each orientation of the RC with respect to the field direction and then average over all orientations of the RCs to determine the "observed yield," $\Phi_T^{obs}(H,\eta)$, for a probe beam at 870 nm whose electric unit vector, $\hat{E}$, is at the angle η to the field direction:

$$\Phi_T^{obs}(H,\eta) = (3/8\pi^2)\int_0^{2\pi}\int_0^{\pi}\int_0^{2\pi}[\hat{E}(\eta)\cdot\hat{\mu}_{870}(\alpha,\beta)]^2 \times \Phi_T(H,\beta,\gamma)\, d\alpha \sin\beta\, d\beta\, d\gamma. \quad [6]$$

The average quantum yield, $\Phi_T^{av}(H)$, and the yield anisotropy, a(H), are then:

$$\Phi_T^{av}(H) = (1/3)[\Phi_T^{obs}(H,0°) + 2\,\Phi_T^{obs}(H,90°)], \quad [7]$$

$$a(H) = \frac{\Phi_T^{obs}(H,0°) - \Phi_T^{obs}(H,90°)}{\Phi_T^{obs}(H,0°) + 2\,\Phi_T^{obs}(H,90°)}. \quad [8]$$

Molecular Triplet Quantum Yield, $\Phi_T(H,\beta,\gamma)$. In order to obtain $\Phi_T(H,\beta,\gamma)$, we first consider the spin Hamiltonian governing the spin dynamics of $P^{+}I^{-}$:

$$\mathcal{H} = \vec{S}_1\cdot\left(\mathbf{g}_1\cdot\vec{H}\beta_e + \sum_i \mathbf{A}_{i1}\cdot\vec{I}_{i1}\right) + \vec{S}_2\cdot\left(\mathbf{g}_2\cdot\vec{H}\beta_e + \sum_i \mathbf{A}_{i2}\cdot\vec{I}_{i2}\right) + J\vec{S}_1\cdot\vec{S}_2 + \vec{S}_1\cdot\mathbf{D}\cdot\vec{S}_2 + \sum_{i,j}\gamma_{ij}\hbar\vec{I}_{ij}\cdot\vec{H} + \sum_{i,j}\vec{I}_{ij}\cdot\mathbf{P}_{ij}\cdot\vec{I}_{ij}, \quad [9]$$

where $\vec{S}_1$ and $\vec{S}_2$ and $\mathbf{g}_1$ and $\mathbf{g}_2$ are the angular momentum operators and g tensors for electrons 1 and 2 on radicals P^{+} and I^{-}, respectively. $\mathbf{A}_{ij}$, $\mathbf{P}_{ij}$, $\vec{I}_{ij}$, and γ_{ij} are, respectively, the hyperfine tensor, quadrupole tensor, angular momentum operator, and magnetogyric ratio for the ith nucleus on the jth radical. J and $\mathbf{D}$ are, respectively, the isotropic exchange coupling constant and the dipole–dipole tensor for the unpaired electron on P^{+} interacting with the unpaired electron on I^{-}. β_e is the Bohr magneton. In order to obtain a simpler expression appropriate for high field, we can make the approximation that the g factor anisotropies are small (very reasonable for π radicals like P^{+} and I^{-}) and neglect terms which couple states split by the large electron Zeeman interaction. In that case the electron spins are quantized in the field and only S and T_0 states mix. If we further neglect the nuclear Zeeman and nuclear quadrupole interactions,* nuclear states are not mixed, and we obtain the following useful form of the high field Hamiltonian for the kth nuclear state:

$$\mathcal{H}'_k = [g\beta_e H + \sum_i \mathbf{A}_{i2}(\beta,\gamma)m_{i2}^k]\,S_z + 3/4\,\mathbf{D}_{zz}(\beta,\gamma)\,S_z^2 + (1/2)\Delta E(\beta,\gamma)\,\vec{S}^2 + \hbar\omega_k(H,\beta,\gamma)\,S_{1z}, \quad [10]$$

where

$$\Delta E(\beta,\gamma) = J - 1/2\,\mathbf{D}_{zz}(\beta,\gamma),$$

$$\omega_k(H,\beta,\gamma) = 1/\hbar\left[\Delta g(\beta,\gamma)\beta_e H + \sum_i \mathbf{A}_{i1}(\beta,\gamma)m_{i1}^k - \sum_i \mathbf{A}_{i2}(\beta,\gamma)m_{i2}^k\right],$$

$$\vec{S} = \vec{S}_1 + \vec{S}_2,\ g = (\mathbf{g}_2)_{zz},\ \Delta g(\beta,\gamma) = (\mathbf{g}_1 - \mathbf{g}_2)_{zz},$$

$$\mathbf{A}_{ij}(\beta,\gamma) = |\hat{z}\cdot\mathbf{A}_{ij}|,\ \mathbf{D}_{zz}(\beta,\gamma) = (\mathbf{D})_{zz},$$

and m_{ij}^k is the quantum number of angular momentum in the direction of the effective hyperfine field, $\hat{z}\cdot\mathbf{A}_{ij}$, for nucleus i on radical j in the kth nuclear spin state.

The radical pair is born in the singlet state, S, and $\mathcal{H}'_k$ can only mix S and T_0 states. This mixing is determined by the energy splitting, $\Delta E(\beta,\gamma)$, and by the coupling constant, $\omega_k(H,\beta,\gamma)$, which is the frequency of S–T_0 mixing in the absence of an energy splitting. In addition to this mixing, the singlet and triplet

---

* Neither the nuclear Zeeman nor the nuclear quadrupole interactions couple singlet and triplet electron spin states directly. However, they can modify the effective hyperfine coupling by mixing nuclear states. With isotropic hyperfine interactions the nuclear Zeeman interaction has no effect, but with anisotropic hyperfine interactions the effective hyperfine coupling may be modified at very high fields. However, in the case discussed here, the contribution of the hyperfine interactions to the yield anisotropy at such fields is small compared to that of the anisotropic difference g tensor; so, the approximation is reasonable.

The nuclear quadrupole interaction only occurs here for the ^{14}N nuclei. When the hyperfine field direction, $\hat{z}\cdot\mathbf{A}_{ij}$, coincides with a principal axis of the quadrupole tensor (e.g., $\hat{x}_P$), the hyperfine-induced coupling is accentuated by the deviation of the quadrupole tensor from axiality in that direction (13).

$$\mathbf{A}_{ij}(\beta,\gamma) = [|\hat{z}\cdot\mathbf{A}_{ij}|^2 + (P_z - P_y)^2]^{1/2}.$$

An extension of the analysis presented below to include a quadrupole tensor modeled on the known nuclear quadrupole transitions in pyridine ($\hat{z}_P\cdot\hat{z}_A = 0$; $P_z/g_e\beta_e = 0.8$ G) (14) shows that neither the maximum $A(\beta,\gamma)$ (Eq. 13, obtained with $\hat{z}$ parallel to $\hat{z}_A$) nor the minimum $A(\beta,\gamma)$ (obtained with $\hat{z}$ perpendicular to $\hat{z}_A$) changes by more than 1%. The exact angular dependence of $A(\beta,\gamma)$ will be changed. The anisotropy of the triplet yield should be only weakly affected.

radical pair states are drained by recombination reactions (rate constants k_S and k_T, Fig. 1). Under these influences, the molecular triplet quantum yield, $\Phi_T(H,\beta,\gamma)$, can be obtained from the stochastic Liouville equation (5, 8). The result, similar to that in ref. 5 and written here in a modified form, is:

$$\Phi_T(H,\beta,\gamma) = \frac{k_T}{k_S + k_T}\left(\frac{1}{N}\sum_{k=1}^{N}\frac{1}{1+[\kappa(\beta,\gamma)/\omega_k(H,\beta,\gamma)]^2}\right) \quad [11]$$

where $\kappa^2(\beta,\gamma) = k_S k_T\{1 + [2\Delta E(\beta,\gamma)/\hbar(k_S + k_T)]^2\}$.

Until this point the derivation is quite general for the high-field limit. We now consider physically reasonable values for the magnitude of each anisotropic magnetic interaction in the particular case of $P^{+}I^{-}$ and the manner in which each affects the yield.

Dipole–Dipole Interaction. Based on a detailed analysis of $\Phi_T(H)$ at low field (0–1,000 G), we have suggested that the zero field splitting parameters for the electron dipole–electron dipole interaction between P^{+} and I^{-} are: $D/g_e\beta_e \approx -40$ to -60 G and $E/g_e\beta_e \approx 10$–15 G (15). In the present analysis, we will consider $D/g_e\beta_e = -45$ G and $E/g_e\beta_e = 10$ G. The required component of the dipole–dipole tensor is then:

$$D_{zz}(\beta,\gamma) = 2D[(\hat{z}\cdot\hat{z}_D)^2 - 1/3] + 2E[(\hat{z}\cdot\hat{x}_D)^2 - (\hat{z}\cdot\hat{y}_D)^2]. \quad [12]$$

$\hat{z}\cdot\hat{z}_D$, $\hat{z}\cdot\hat{x}_D$, and $\hat{z}\cdot\hat{y}_D$ are the projections of the principal axes of the dipole–dipole tensor on the applied field direction $\hat{z}$. They are functions of the Euler angles β, γ, α_D, β_D, and γ_D. Neither the precise magnitude nor the sign of the isotropic exchange interaction, J, is known at this time, although it is certainly quite small (7, 8). The value of J does affect the way in which the dipolar interaction contributes to the yield anisotropy. For simplicity we will assume J = 0 here. The dipolar energy splitting of S and T_0 is greatest with the field along $\hat{z}_D$ (approximately the direction joining the two radicals). If we could ignore the other anisotropic interactions, the most negative yield anisotropy would occur for $\hat{z}_D$ parallel to $\hat{\mu}_{870}$ ($\beta_D = 0°$), and the most positive anisotropy, for $\hat{y}_D$ parallel to $\hat{\mu}_{870}$ ($\beta_D = 90°$, $\gamma_D = 90°$).

Anisotropic Nuclear Hyperfine Interactions. Consideration of the hyperfine interactions in both P^{+} and I^{-} (16) shows that the two nitrogens in the reduced rings of I^{-} should have by far the dominant anisotropic hyperfine interactions; thus, we take the other hyperfine interactions to be isotropic. The isotropic ^{14}N hyperfine coupling constants in the bacteriopheophytin *a* anion are $A_N/g_e\beta_e = +2.3$ G and the spin density is calculated to be 0.10 on each of these nitrogens (17). From this spin density we calculate an approximate anisotropic coupling constant, $B_N/g_e\beta_e = +1.7$ G (13). The three principal values of the axial ^{14}N hyperfine tensor are given by:

$$A_x/g_e\beta_e = A_y/g_e\beta_e = (A_N - B_N)/g_e\beta_e = 0.6 \text{ G}$$

and

$$A_z/g_e\beta_e = (A_N + 2B_N)/g_e\beta_e = 5.7 \text{ G}.$$

In order to calculate the quantum yield, we must consider both the isotropic and anisotropic hyperfine contributions. Due to the large number of nuclear hyperfine interactions in the radical pair, $P^{+}I^{-}$, we replace the sum over discrete nuclear states in Eq. 11 with an integration over a gaussian distribution for ω_k centered at $\Delta g(\beta,\gamma)\beta_e H/\hbar$ with second moment, $[A(\beta,\gamma)/2\hbar]^2$, where:

$$A^2(\beta,\gamma) = A_1^2 + A_2^2 + 2(4/3)I_N(I_N+1)(A_z^2 - A_x^2)[(\hat{z}\cdot\hat{z}_A)^2 - 1/3] \quad [13]$$

The first term is the contribution from the nuclei on P^{+}; $A_1/g_e\beta_e$ has been measured by EPR to be 9.8 G (18). The second term is the contribution from the nuclei on I^{-}; $A_2/g_e\beta_e$ has been measured by EPR to be 13 G (18). The third term represents the correction to the second term due to the two anisotropic nitrogen hyperfine interactions in I^{-}, which have common principal values and axes. I_N is the total spin quantum number of ^{14}N ($I_N = 1$); $\hat{z}\cdot\hat{z}_A$ is the projection of the principal z_A axis of these hyperfine interactions on the field direction. $A(\beta,\gamma)$ is greatest with the field along $\hat{z}_A$. If we could ignore the other anisotropic interactions, the most positive yield anisotropy would occur if $\hat{\mu}_{870}$ were parallel to the common z_A axis of the hyperfine tensors of these two nitrogens; that is, if $\hat{\mu}_{870}$ were perpendicular to the molecular plane of I^{-} ($\beta_A = 0°$). Conversely, the most negative yield anisotropy would occur if $\hat{\mu}_{870}$ were parallel to the plane of I^{-} ($\beta_A = 90°$).

***g* Factor Anisotropy.** For generality, we take the difference *g* tensor to be made up of an isotropic component, Δg_{iso}, an axial component, Δg_{ax}, and a rhombic component, Δg_{rh}, such that its principal values are:

$$\Delta g_x = \Delta g_{iso} - \Delta g_{ax} - \Delta g_{rh}$$

$$\Delta g_y = \Delta g_{iso} - \Delta g_{ax} + \Delta g_{rh}$$

$$\Delta g_z = \Delta g_{iso} + 2\Delta g_{ax}.$$

The required component of the difference *g* tensor is then given by:

$$\Delta g(\beta,\gamma) = \Delta g_{iso} + \Delta g_{ax}[3(\hat{z}\cdot\hat{z}_g)^2 - 1] - \Delta g_{rh}[(\hat{z}\cdot\hat{x}_g)^2 - (\hat{z}\cdot\hat{y}_g)^2], \quad [14]$$

where $\hat{z}\cdot\hat{z}_g$, $\hat{z}\cdot\hat{x}_g$, and $\hat{z}\cdot\hat{y}_g$ are the projections of the principal axes of the difference tensor $\Delta\mathbf{g}$ on the field direction, $\hat{z}$.

The *g* factors which have been measured for trapped P^{+} and I^{-} (18) give $\Delta g_{iso} = -1.0 \times 10^{-3}$, consistent with the value obtained from our previous, isotropic analysis of the triplet yield (5). Organic radicals have only very minor *g* tensor anisotropies, with principal values deviating from the *g* factor of the free electron, 2.0023, by amounts on the order of 10^{-3} (13). Δg_{ax} and Δg_{rh} are expected to be of this order of magnitude. As an example, consider the effect of $\Delta g_{ax} < 0$ with $\Delta g_{rh} = 0$. $|\Delta g(\beta,\gamma)|$ is greatest with the field along $\hat{z}_g$. If we could ignore the other anisotropic interactions, for $\hat{z}_g$ parallel to $\hat{\mu}_{870}$ ($\beta_g = 0°$), a(H) would increase from zero with increasing field to a positive maximum and decrease back to zero at extremely high fields. Conversely, for $\hat{z}_g$ perpendicular to $\hat{\mu}_{870}$ ($\beta_g = 90°$), a(H) would decrease from zero to a negative minimum and return to zero at extremely high fields. a(H) is expected to approach zero at extremely high fields in all cases because there the rate of S–T_0 mixing is so rapid for all orientations that the states are in quasi-equilibrium, and $\Phi_T(\beta,\gamma) = k_T/(k_S + k_T)$.

Modeling of Data. In order to show that the experimental data in Fig. 2 are consistent with reasonable values of the magnetic parameters discussed above, $\Phi_T^{av}(H)$ and a(H) are calculated as follows. The average of $[\hat{E}(\eta)\cdot\hat{\mu}_{870}(\alpha,\beta)]^2$ over the Euler angle α is obtained analytically. For a given orientation of the RC axis system (β and γ), the values of $\Delta E(\beta,\gamma)$, $A(\beta,\gamma)$, and $\Delta g(\beta,\gamma)$ are calculated by using Eqs. 12–14. $\Phi_T(H,\beta,\gamma)$ is then calculated by using Eq. 11 with numerical integration over ω as described above. Eq. 6 is then numerically integrated over β and γ.

The results of such calculations are shown in Fig. 3 for the parameters listed in the legend. Our purpose is to show that the experimental field dependence of the yield and its anisotropy can be explained by anisotropic magnetic interactions in

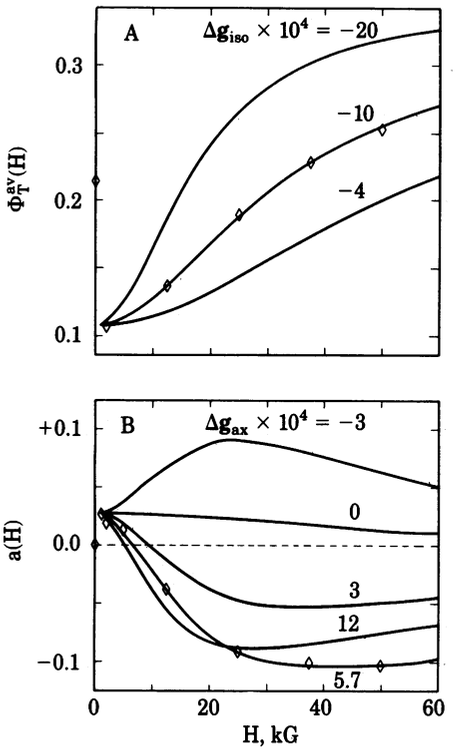

FIG. 3. (*A*) Calculated (——) and experimental (◇) average quantum yields, $\Phi_T^{av}(H)$, as a function of magnetic field. Curves were calculated for a standard set of parameters (below), except for Δg_{iso}. Experimental values are based on $\Phi_T(0) = 0.21$ (9). (*B*) Calculated (——) and experimental (◇) quantum yield anisotropies, a(H), as a function of magnetic field. Curves were calculated for a standard set of parameters (below), except for Δg_{ax}. Standard set of parameters: kinetic, $k_S = 6.5 \times 10^7\ s^{-1}$; $k_T = 3.5 \times 10^7\ s^{-1}$; S–$T_0$ splitting, J = 0, $D/g_e\beta_e = -45$ G, $E/g_e\beta_e = 10$ G, $\alpha_D = 0°$, $\beta_D = 90°$, $\gamma_D = 40°$; hyperfine tensor, $A_1/g_e\beta_e = 9.8$ G, $A_2/g_e\beta_e = 13.0$ G, $A_z/g_e\beta_e = 5.7$ G, $A_x/g_e\beta_e = A_y/g_e\beta_e = 0.6$ G, $\alpha_A = 0°$, $\beta_A = 73°$; *g* tensor, $\Delta g_{iso} = -1 \times 10^{-3}$, $\Delta g_{ax} = 5.7 \times 10^{-4}$, $\Delta g_{rh} = 0$, $\alpha_g = 0°$, $\beta_g = 0°$, $\gamma_g = 0°$.

the radical pair when reasonable values are used for the parameters. In particular, these calculated curves demonstrate the strong dependence of the yield and anisotropy on Δg_{iso} and Δg_{ax}, respectively. The dependence on the other parameters, such as k_S, k_T and J, as well as a discussion of the low-field behavior (H < 500 G) are presented elsewhere (9, 15). Here we discuss those parameters that make a large contribution to the anisotropy.

At moderate fields (H ≈ 1,000 G), Δg plays no role in determining the yield or anisotropy; however, both the dipole–dipole and anisotropic hyperfine interactions can make a contribution. Many sets of the angles α_D, β_D, γ_D, α_A, and β_A can fit the data. As the magnetic field is increased, the rate of S–T_0 mixing increases due to Δg_{iso}, and the effects of the dipolar and hyperfine interactions on the yield and anisotropy decrease (see Fig. 3*B* with $\Delta g_{ax} = 0$).

The effects of Δg_{rh} (not shown in Fig. 3) are similar to those of Δg_{ax}, except that different angles are needed to obtain the observed a(H). In either case, a(H) decreases from the positive value determined by the other interactions at moderate fields, reaches a minimum near 50 kG, and returns to zero at higher field. It would be valuable to measure a(H) beyond 50 kG to verify this. The position of this minimum is a sensitive function of the *g* tensor anisotropy. Large absolute magnitudes of Δg_{ax} or Δg_{rh} can be ruled out as seen for Δg_{ax} in Fig. 3. Furthermore, the large negative anisotropy observed at high fields can only be accounted for with $\hat{\mu}_{870}$ along a principal axis of the difference *g* tensor and with the principal value along that axis near zero.

In summary, the magnetic field-dependent anisotropic triplet quantum yield in quinone-depleted RCs offers an approach for examining the three-dimensional arrangement of the reactive components. The anisotropy of the quantum yield is positive at low field and negative at high field. Three types of magnetic interactions in the primary radical ion-pair intermediate are expected to contribute: the electron dipole–electron dipole and anisotropic nuclear hyperfine interactions at lower fields and the anisotropic *g* tensor at high field. The absolute magnitude of the contribution of each effect depends on the magnitudes of the components of the anisotropic tensors and the geometrical relationship of the principal axes to the transition dipole moment used to detect the yield. We have shown that the data can be modeled with reasonable values of these parameters. These data, combined with photoselected EPR experiments on P^+, I^-, and P^+I^-, may help to answer some of the basic structural questions posed at the start of this paper.

We thank the Varian Corporation for lending us the superconducting magnet used in these experiments. This work was supported by the National Science Foundation (PCM7926677) and the Science and Education Administration of the U.S. Department of Agriculture (78-59-2066-0-1-147-1). C.E.D.C. is a National Science Foundation Predoctoral Fellow; S.G.B. is an Alfred P. Sloan and Camille and Henry Dreyfus Teacher-Scholar.

1. Thurnauer, M. C., Katz, J. J. & Norris, J. R. (1975) *Proc. Natl. Acad. Sci. USA* **72**, 3270–3274.
2. Bowman, M. K., Budil, D. E., Closs, G. L., Kostka, A. G., Wraight, C. A. & Norris, J. R. (1981) *Proc. Natl. Acad. Sci. USA* **78**, 3305–3307.
3. Hoff, A. J., Rademaker, H., van Grondelle, R. & Duysens, L. N. M. (1977) *Biochim. Biophys. Acta* **460**, 547–554.
4. Blankenship, R. E., Schaafsma, T. J. & Parson, W. W. (1977) *Biochim. Biophys. Acta* **461**, 297–305.
5. Chidsey, C. E. D., Roelofs, M. G. & Boxer, S. G. (1980) *Chem. Phys. Lett.* **74**, 113–118.
6. Boxer, S. G., Chidsey, C. E. D. & Roelofs, M. G. (1982) *J. Am. Chem. Soc.* **104**, 1452–1454.
7. Werner, H.-J., Schulten, K. & Weller, A. (1978) *Biochim. Biophys. Acta* **502**, 255–268.
8. Haberkorn, R. & Michel-Beyerle, M. E. (1979) *Biophys. J.* **26**, 489–498.
9. Roelofs, M. G. (1982) Dissertation (Stanford Univ., Stanford, CA).
10. Butler, W. F., Johnston, D. C., Shore, H. B., Fredkin, D. R., Okamura, M. Y. & Feher, G. (1980) *Biophys. J.* **32**, 967–992.
11. Schenck, C. C., Blankenship, R. E. & Parson, W. W. (1982) *Biochim. Biophys. Acta* **680**, 44–59.
12. Edmonds, A. R. (1974) *Angular Momentum in Quantum Mechanics* (Princeton Univ. Press, Princeton, NJ), p. 6.
13. Gordy, W. (1980) *Theory and Applications of Electron Spin Resonance* (Wiley, New York).
14. Guibé, L. & Lucken, E. A. C. (1968) *Mol. Phys.* **14**, 79–87.
15. Roelofs, M. G., Chidsey, C. E. D. & Boxer, S. G. (1982) *Chem. Phys. Lett.* **87**, 582–588.
16. Hoff, A. J. (1979) *Phys. Rep.* **54**, 75–200.
17. Fajer, J., Forman, A., Davis, M. S., Spaulding, L. D., Brune, D. C. & Felton, R. H. (1977) *J. Am. Chem. Soc.* **99**, 4134–4140.
18. Feher, G. & Okamura, M. Y. (1978) in *The Photosynthetic Bacteria*, eds. Clayton, R. K. & Sistrom, W. R. (Plenum, New York), pp. 349–386.